



Corrosion resistance of multilayer and gradient coatings deposited by PVD and CVD techniques

L.A. Dobrzański*, K. Lukaszewicz, D. Pakuła, J. Mięka

Division of Materials Processing Technology, Management and Computer Techniques in Materials Science, Institute of Engineering Materials and Biomaterials, Silesian University of Technology, ul. Konarskiego 18a, 44-100 Gliwice, Poland

* Corresponding author: E-mail address: leszek.dobrzanski@polsl.pl

Received 15.11.2006; accepted in revised form 25.01.2007

ABSTRACT

Purpose: The aim of the research was the investigation of the corrosion resistance and structure of the TiN, TiN+multiTiAlSiN+TiN, TiN+TiAlSiN+TiN, TiN+TiAlSiN+AlSiTiN coatings deposited by PVD process and Ti(C,N)+TiN, Ti(C,N)+Al₂O₃+TiN, TiC+TiN, TiC+Ti(C,N)+Al₂O₃+TiN, TiN+Al₂O₃ coatings deposited by CVD process.

Design/methodology/approach: Investigation of the electrochemical corrosion behavior of the samples in a PGP 201 Potentiostat/Galvanostat, in a three-electrode chamber, the metallographic examinations (SEM), the examinations of thin foils (TEM), texture analysis was done.

Findings: It was found out that coatings deposited by PVD and CVD method display high corrosion resistance. The best results were obtained for the TiN+multiTiAlSiN+TiN coatings deposited by PVD process and TiC+Ti(C,N)+Al₂O₃+TiN coatings deposited by CVD process.

Practical implications: The obtained results are the basis for the optimization of corrosion resistance of the PVD and CVD coatings deposited onto the substrate made from tool materials.

Originality/value: The paper presents the influence of the coatings technology and of the number of layers on the corrosion resistance.

Keywords: Corrosion; PVD; CVD; Ceramic tools materials

PROPERTIES

1. Introduction

The dynamical development of the industry poses higher and higher demands, especially in the area of the adjustment of the properties of materials to their operation conditions or applications. This regards, first of all, constructional materials, tool materials, etc. Achievement of the required high working properties is connected, in most cases, with the necessity of improvement of their manufacturing technologies, employment of novel manufacturing technologies or modifications of the surface

layer. Deposition of hard coatings (transition metal nitrides, carbides or oxides) on material surface by PVD and CVD processes features one of the most intensely developed directions of improvement of the working properties of materials [1-3]. This technology makes it possible to modify their surface by shaping their physical and chemical properties.

One of the general reasons for depositing by PVD techniques is developing the protective coating presenting corrosion resistance higher than the substrate [4-12]. Ceramic hard coatings increase of the life of the coated components, not only due to the protection against aggressive environments, but also

during operation involving mechanical contact with abrasive surfaces. This effect results of high hardness resulting from the smaller grain size of the coatings' structure [13-19].

The goal of this work is to investigate corrosion resistance of coatings deposited by PVD and CVD techniques.

2. Experiments

The investigations were carried out on the multi-point inserts made from the Si_3N_4 nitride ceramics uncoated and coated in the PVD and CVD process with thin coatings. The inserts made from Si_3N_4 were multilayer coated in the PVD process – Cathodic Arc Evaporation (CAE). Specifications of the investigated materials are presented in Table 1.

Table 1.
Characteristics of the PVD and CVD coatings deposited on the Si_3N_4 nitride ceramics

Type	Coating Composition	Coating thickness, (μm)	Process type
mono layer	TiN	0.8	PVD
multilayer	TiN+multiTiAlSiN+TiN	4.0	PVD
gradient/multilayer	TiN+TiAlSiN+TiN	2.0	PVD
gradient	TiN+TiAlSiN+AlSiTiN	2.5	PVD
two layers	Ti(C,N)+TiN	4.2	CVD
multilayer	Ti(C,N)+ Al_2O_3 +TiN	9.5	CVD
two layers	TiC+TiN	5.4	CVD
multilayer	TiC+Ti(C,N)+ Al_2O_3 +TiN	7.8	CVD
two layers	TiN+ Al_2O_3	10.0	CVD

*commercially available inserts from various manufacturers

Investigation of the electrochemical corrosion behaviour of the samples was done in a PGP 201 Potentiostat/Galvanostat, in a three-electrode chamber using a 1 M NaOH solution. The auxiliary and reference electrodes were platinum and calomel respectively. The following tests were performed:

- measurements of the polarization in the range of -500 (-800) mV to 500 mV at the scanning rate of 15 mV/min, to determine the corrosion current i_{cor} on the substrate using the Tafel analysis method and VoltaMaster 4 software package;
- measurements of the corrosion potential E_{cor} during 60 minutes;
- measurement of the corrosion rate.

Observations of the investigated coatings' structures were carried out on the transverse fractures on the scanning electron microscope (SEM) Philips XL-3. To obtain the fracture images the Secondary Electrons (SE) and the Back Scattered Electrons (BSE) detection methods were used with the accelerating voltage in the range of 15-20 [kV], maximum magnifications are 10000 \times . The specimens with notches cut on them were cooled in liquid

nitrogen. Topography of the investigated coatings' surfaces was also examined on the scanning electron microscope.

The diffraction examinations and examinations of thin foils were made on the JEOL JEM 3010UHR transmission electron microscope at the accelerating voltage of 300 kV and maximum magnification 300000 \times . The diffraction patterns from the transmission electron microscope were solved using the computer program. Thin foils were made in the longitudinal and transverse sections from the 0.2-0.5 mm thick laminae cut from the solid specimens, from which 3 mm O.D. disks were cut out, with the initially ground and levelled surfaces. The lamellae were next mechanically thinned on the Disc Grinder to thickness of about 80 μm and ion polished using the Gatan firm equipment.

The Seifert-FPM XRD 7 X-ray diffractometer, equipped with the texture add-on, was used for evaluation of the coatings' structures. The X-ray radiation was used of the Co $K\alpha$ cobalt lamp with the 35 kV supply voltage and current of 40 mA. Analysis of the investigated coatings texture was made using the inverse pole figures method. Intensity of the (111), (002), (022) and (113) diffraction lines was analysed – in case of the TiC, TiN and Ti(C,N) phases, and of the (012), (104), (110), (113), (116), (030), and (1010) ones in case of the Al_2O_3 phase. The line intensity was measured after the graphical separation of the overlaying lines and after isolating the clear profile of the analysed line. The measured line intensity was divided by the relative intensity of this line specified in the catalogues, and in case of the Ti(C,N) phase diffraction lines – by the value interpolated using the TiC and TiN catalogue values. Basing on these values and on location of traces normal to the (001), (011), (111) and (113) planes – the equal density isolines of spatial distribution of the normal direction to the sputtered plane (KN) were plotted in the base triangle. Further, the figures were normalized to make determining the isolines values possible in units being multiples of density for the uniform distribution in the space that is for the specimen that does not reveal texture. This made it possible to assess how strongly the investigated specimens are textured.

3. Discussion of results

It was found out, as a result of the electrochemical corrosion investigations, that the lowest corrosion current density i_{cor} ; and therefore, the lowest anode dissolving of the coating and the best corrosion protection properties are obtained for the TiN+multiTiAlSiN+TiN coatings deposited by PVD process and TiC+Ti(C,N)+ Al_2O_3 +TiN coatings deposited by CVD process. (Fig. 1,2, Table 2). This may be explained by the fact that the multilayer coating deposition system gives better possibility to prevent corrosion causes, like scratches or crevices. Small pores and cracks in the coating and the difference between the big cathode area (coating) and the small anode surface (bottom of pores) decreases the corrosion protection of coatings. Defects and failures occurring in a single layer in the deposition process may be neutralised or "masked" by the successively deposited coating layers. Therefore, the corrosive agent path is extended or blocked. That is why with multilayers coating the corrosive agent needs more time to penetrate through coating defects into the substrate material, than in case of monolayers coating. The current density

of monolayer coatings is much higher than that one obtained for multilayer coatings. Corrosion currents and corrosion rate can be determined from the polarisation curves flow, as well as with the Volta Master software (Table 2).

Results of the corrosion potential E_{cor} confirm the high corrosion resistance of the coatings (Figs. 3,4, Table 2). The relatively high initial potential for some coatings is explained by the need of longer time for reaching by the NaOH solution to the substrates of specimens by diffusion through small surface defects.

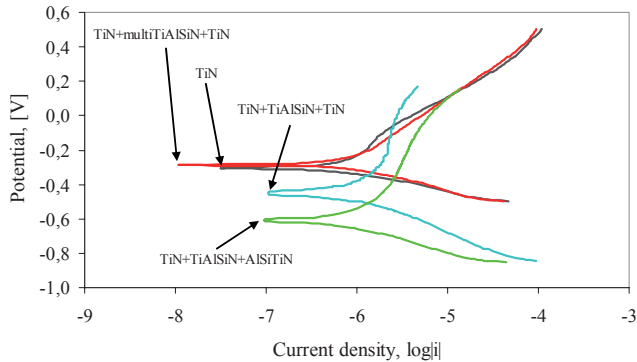


Fig. 1. Potentiodynamic polarization curves of the coatings deposited by PVD process in 1 M NaOH solution

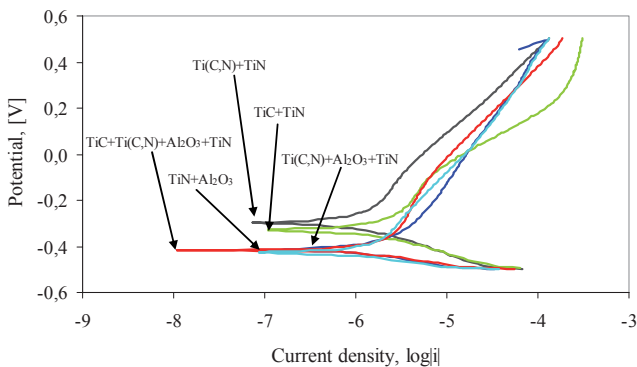


Fig. 2. Potentiodynamic polarization curves of the coatings deposited by CVD process in 1 M NaOH solution

Impedance measurement values (Table 2) shows that the coatings play role of the diffusion barrier. The multilayer coatings have the best protective properties which are also confirmed by the polarisation examination results.

On the basis of the metallographic research done with the use of the scanning electron microscope, it was stated that all coatings formed both in the high temperature CVD process as well as the PVD one, were characterised by laminar arrangement. All layers of the coating adhere to each other as well as to the nitride ceramics substrate. The coatings are also characterised by the uniform structure without any visible cracks and pinholes. The surface of the

CVD coatings used in the tests is not uniform. All these coatings indicate surface defects in the form of pinholes, cracks and fractures typical of coatings formed in the CVD process. The surface topography of the PVD coatings is likewise heterogeneous. The lack of uniformity is caused by the micro molecules which appear on the coating's surface as the result of spattering of drops during the coating deposition (Fig. 5).

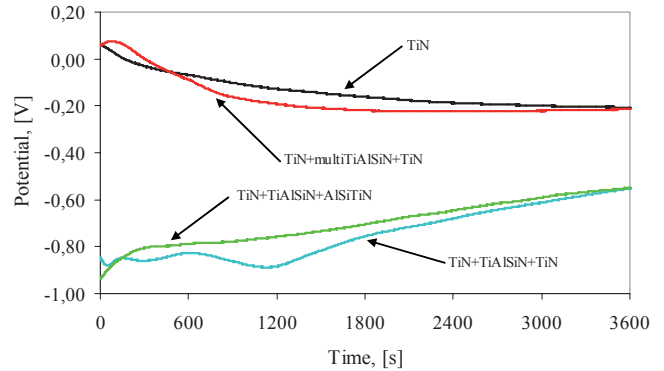


Fig. 3. Open circuit potential curves of the coatings deposited by PVD process in 1 M NaOH solution

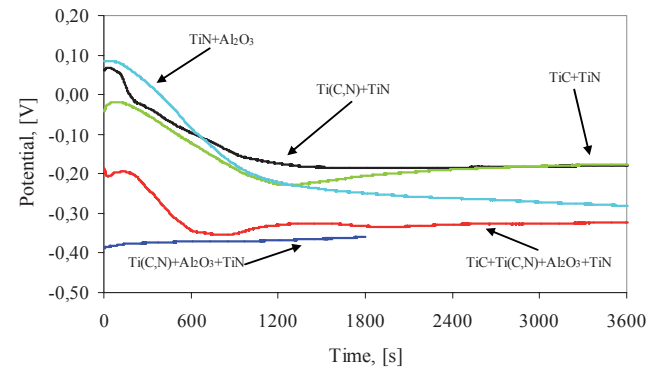


Fig. 4. Open circuit potential curves of the coatings deposited by CVD process in 1 M NaOH solution

Examinations of thin foils carried out both in parallel to the surface of the investigated $TiN+Al_2O_3$ coating confirm that the coating containing phases of the TiN and Al_2O_3 types was deposited onto the substrate from the tool nitride ceramics. The structure of the Al_2O_3 layer with the trigonal lattice is characterised in the parallel section by fine grains with grain size not exceeding 500 nm (Fig. 6).

In case of texture of the investigated coatings on the nitride ceramics, when the particular phase was deposited in several layers, the presented pole figures should be treated as the averaged figures for all layers of that phase; however, bearing in mind that it is not an arithmetic average: the outer layer has the biggest effect on the pole figure of the particular phase. This is not that important, assuming that texture of all layers is similar.

Table 2.

Summary results of the electrochemical corrosion investigation

Coating type	Current density i_{cor} , ($\mu\text{A}/\text{cm}^2$)	Corrosion potential E_{cor} , (mV)	Corrosion rate, (mm/year)	Resistance polarization R_p , ($\text{k}\Omega\text{cm}^2$)	Corrosion potential $E(i_{cor}=0)$ (mV)
TiN	0.37	-206	4.66	38.5	-312
TiN+multiTiAlSiN+TiN	0.36	-215	4.14	41.1	-292
TiN+TiAlSiN+TiN	0.47	-342	5.52	65.7	-460
TiN+TiAlSiN+AlSiTiN	0.41	-508	4.88	63.9	-618
Ti(C,N)+TiN	0.48	-179	6.08	31.2	-306
Ti(C,N)+Al ₂ O ₃ +TiN	0.56	-359	6.79	16.3	-418
TiC+TiN	0.73	-176	9.20	17.7	-337
TiC+Ti(C,N)+Al ₂ O ₃ +TiN	0.21	-320	3.11	14.9	-415
TiN+Al ₂ O ₃	0.31	-281	3.74	17.4	-408

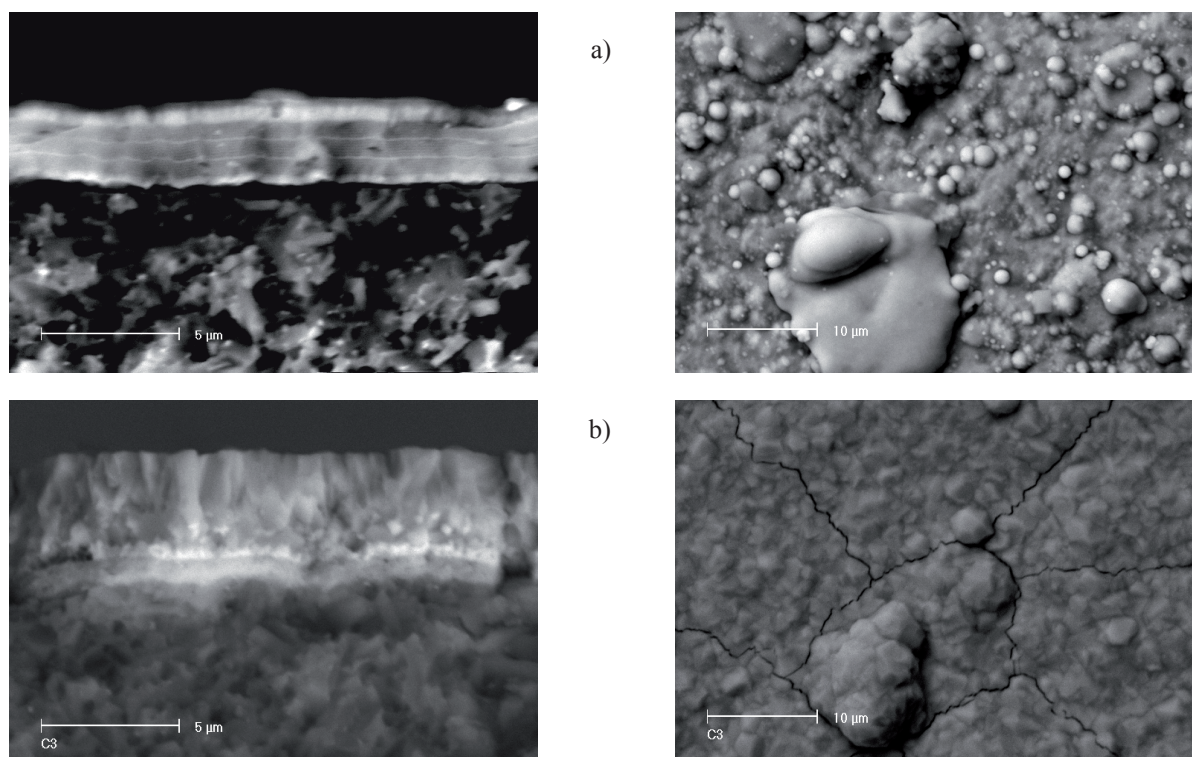


Fig. 5. Fracture surface and topography of the a) TiN+multiTiAlSiN+TiN and b) TiC+TiN coating surface deposited onto the Si₃N₄ nitride ceramics substrate

Most of the pole figures prove that the texture of the TiN layers deposited is very weak. It is especially weak in the specimens with the TiN+multiTiAlSiN+TiN coating, where the density of normals ranges from 0.8 to 1.3 of the density corresponding to the uniform distribution. The distinguished TiN deposition plane, in most cases, is the crystallographic plane from the {111} family, or the {111} + {001} double texture occurs. This is the situation in case of specimens with the TiN+multiTiAlSiN+TiN and Ti(C,N)+Al₂O₃+TiN coatings, where

only the {111} orientation occurs. It is also one of the two distinguished planes – apart from the {001} one – in specimens with the TiN+TiAlSiN+TiN and TiN+TiAlSiN+AlSiTiN coatings. The TiC+Ti(C,N)+Al₂O₃+TiN coating reveals the {001} single texture of the TiN layer; whereas the TiN+Al₂O₃ coating – the {011} single texture. The texture of the TiN layers in the examined material with the TiN+TiAlSiN+TiN and TiN+TiAlSiN+AlSiTiN coatings is relatively strong.

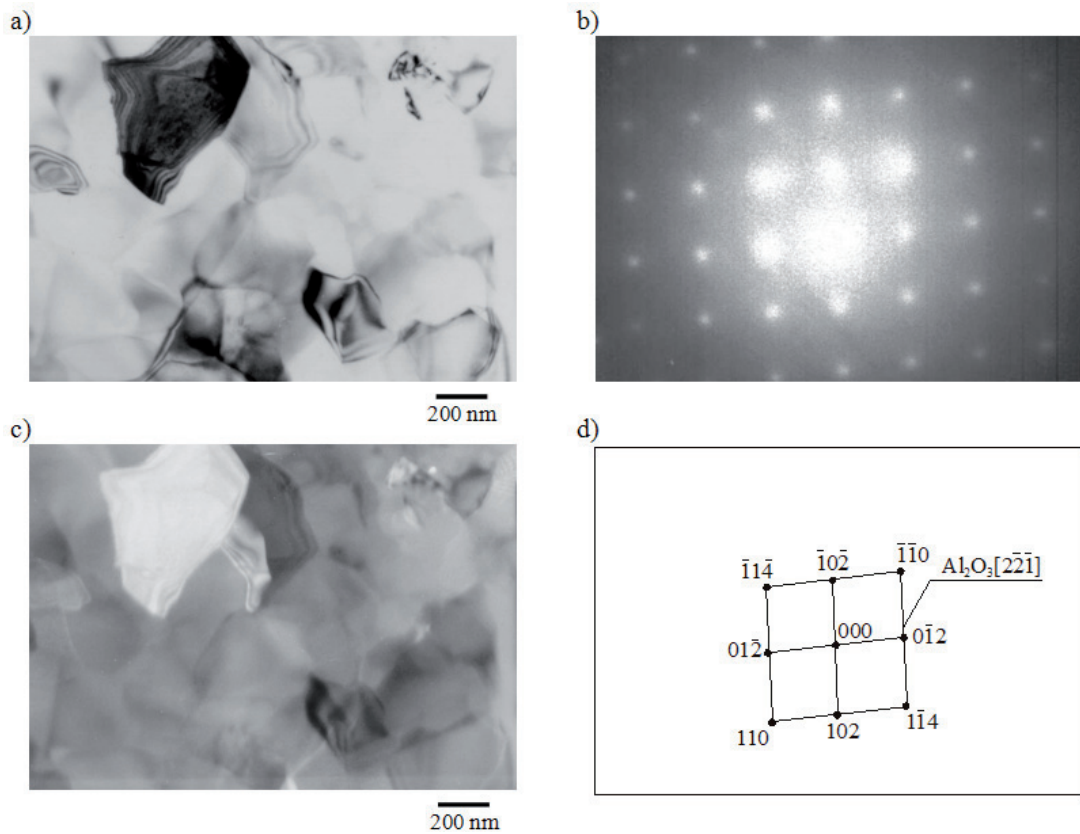


Fig. 6. Structure of TiN+Al₂O₃+TiN+Al₂O₃+TiN coating – layers Al₂O₃; thin foil structure parallel to the layer surface (TEM): a) light field, b) diffraction pattern from the area as in figure a, c) dark field from the(012) reflex Al₂O₃, d) solution of the diffraction pattern from figure b

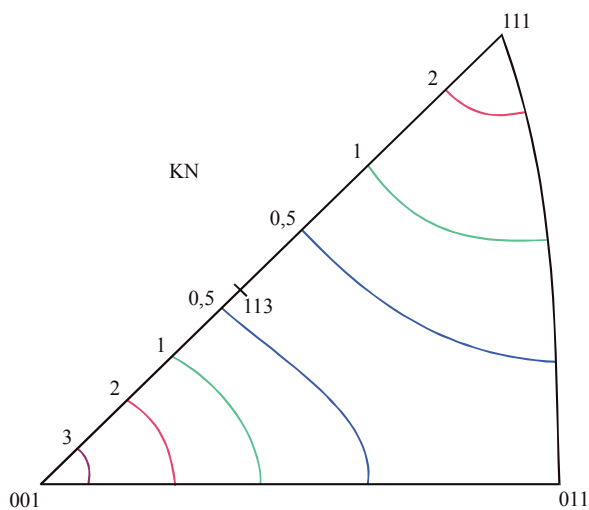


Fig. 7. Exemprary inverse for TiN layer representing the distribution of normal to the TiN+TiAlSiN+AlSiTiN coating surface in the (001)-(011)-(111) base triangle (KN - normal direction)

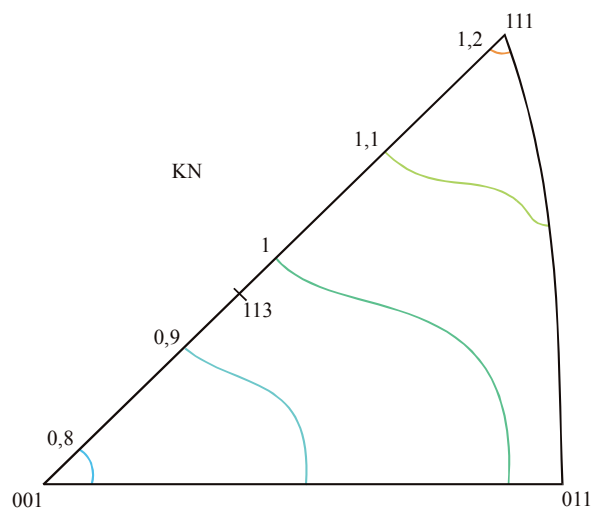


Fig. 8. Exemprary inverse for Ti(C,N) layer representing the distribution of normal to the TiC+Ti(C,N)+Al₂O₃+TiN coating surface in the (001)-(011)-(111) base triangle (KN - normal direction)

The texture is rather weak or very weak in the remaining coatings. Texture of the majority of the Ti(C,N) and TiC layers is also very weak. In case of the TiC+Ti(C,N)+Al₂O₃+TiN coating the density of normals in the pole figures ranges from 0.80 to 1.25. In case of the TiC and Ti(C,N) layers, introduced into the TiC+Ti(C,N)+Al₂O₃+TiN coating, the distinguished deposition plane is the {111} crystallographic plane (Figs. 7,8).

4. Summary

Corrosion current density – corrosion rate - was determined by analysis of the potentiodynamic polarization curves. The corrosion current density for the TiN+multiTiAlSiN+TiN coatings deposited by PVD process is 0.36 $\mu\text{A}/\text{cm}^2$ and TiC+Ti(C,N)+Al₂O₃+TiN coatings deposited by CVD process is 0.21 $\mu\text{A}/\text{cm}^2$, which attests to good anticorrosion properties of the PVD coatings, especially of the multilayer ones. This is connected with better possibilities of corrosion prevention, due to the employment of the multilayered coating deposition in the PVD process. Failures, like pores, crevices or columnar structure occurring in case of the single layer put down in the deposition process may be neutralized by the successively deposited coating layers. In this way, the corrosion agents' path is longer or blocked.

Evaluating differences of textures of the TiN layers obtained with the PVD and CVD methods one can state that - in the most general understanding - the method of physical deposition from the gaseous phase favours development of the relatively strong texture. Also the very weak texture of the carbide and nitrocarbide layers, deposited with the chemical deposition from the gaseous phase method, seems to confirm the rule that this method leads to development of layers with the very weak texture [14, 17].

Acknowledgements

Researches were financed partially within the framework of the Polish State Committee for Scientific Research Project KBN PBZ-100/4/T08/2004 headed by Prof. L.A. Dobrzański and within the framework of the Scholarship No S-096-2005 of the International Visegrad Fund realized by Dr Daniel Pakuła.

Additional information

The presentation connected with the subject matter of the paper was presented by the authors during the 11th International Scientific Conference on Contemporary Achievements in Mechanics, Manufacturing and Materials Science CAM3S'2005 in Gliwice-Zakopane, Poland on 6th-9th December 2005.

References

- [1] L.A. Dobrzański, K. Lukaszewicz, Erosion resistance and tribological properties of coatings deposited by reactive magnetron sputtering method onto the brass substrate, *Journal of Materials Processing Technology* 157-158 (2004) 317-323.
- [2] K. Bobzin, E. Lugscheider, M. Maes, P.W. Gold, J. Loos, M. Kuhn, High-performance chromium aluminium nitride PVD-coatings on roller bearings, *Surface & Coatings Technology* 188-189 (2004) 649-654.
- [3] K. Holmberg, A. Matthews, *Coating Tribology*, Elsevier, Amsterdam, 1994.
- [4] L. Cunha, M. Andritschky, L. Rebouta, K. Pischow, Corrosion of CrN and TiAlN coatings in chloride-containing atmospheres, *Surface & Coatings Technology* 116-119 (1999) 1152-1160.
- [5] L.A. Dobrzański, K. Lukaszewicz, A. Zarychta, L. Cunha, Corrosion resistance of multilayers coatings deposited by PVD techniques onto the brass substrate, *Journal of Materials Processing Technology* 164-165 (2005) 816-821.
- [6] S. Rossi, L. Fedrizzi, M. Leoni, P. Scardi, Y. Massiani, (Ti,Cr)N and Ti/TiN PVD coatings on 304 stainless steel substrates: wear-corrosion behaviour, *Thin Solid Films* 350 (1999) 161-167.
- [7] H.P. Feng, C.H. Hsu, J.K. Lu, Y.H. Shy, Effects of PVD sputtered coatings on the corrosion resistance of AISI 304 stainless steel, *Materials Science and Engineering* 347 (2003) 123-129.
- [8] W. Kajzer, M. Kaczmarek, A. Krauze, J. Marciniak, Surface modification and corrosion resistance of Ni-Ti alloy used for urological stents, *Journal of Achievements in Materials and Manufacturing Engineering* 20 (2007) 123-126.
- [9] S. Kaciulis, A. Mezzi, G. Montesperelli, F. Lamastra, M. Rapone, F. Casadei, T. Valente, G. Gusmano, Multi-technique study of corrosion resistant CrN/Cr/CrN and CrN:C coatings, *Surface & Coatings Technology* 201 (2006) 313-319.
- [10] A. Kagiya, K. Terakado, R. Urao, Effect of nitriding and TiN coating temperatures on the corrosion resistance of the combined surface modification layer, *Surface and Coatings Technology* 169 -170 (2003) 397-400.
- [11] A. Hikmet, S. Sadri, The effect of PVD coatings on the corrosion behaviour of AZ91 magnesium alloy, *Materials and Design* 27 (2006) 1174-1179.
- [12] H. Altun, S. Sen, The effect of PVD coatings on the corrosion behaviour of AZ91 magnesium alloy, *Materials and Design* 27 (2006) 1174-1179.
- [13] S. Karablov, M.A.M. Ibrahim, M. Yoshimura, Hydrothermal corrosion of TiAlN and CrN PVD films on stainless steel, *Corrosion Science* 47 (2005) 1839-1854.
- [14] D. Pakuła, Structure and properties of the multi-layer PVD and CVD wear-resistant coatings on the Si₃N₄ nitride tool ceramics, PhD Thesis, Silesian University of Technology, Faculty of Mechanical Engineering, Gliwice, Poland, 2003, (in Polish).

- [15] L.A. Dobrzański, Engineering Materials and Materials Design, Fundamentals of Materials Science and Physical Metallurgy, WNT, Warszawa, 2006 (in Polish).
- [16] L.A. Dobrzański, D. Pakuła, Structure and properties of the wear resistant coatings obtained in the PVD and CVD processes on tool ceramics, Materials Science Forum 513 (2006) 119-133.
- [17] L.A. Dobrzański, D. Pakuła, Comparison of the structure and properties of the PVD and CVD coatings deposited on nitride tool ceramics, Journal of Materials Processing Technology, 164-165 (2005) 832-842.
- [18] L.A. Dobrzański, L. Wosińska, K. Gołombek, J. Mikuła, Structure of multicomponent and gradient PVD coatings deposited on sintered tool materials, Journal of Achievements in Materials and Manufacturing Engineering 20 (2007) 99-102.
- [19] L.A. Dobrzański, D. Pakuła, J. Mikuła K. Lukaszewicz, Corrosion resistance of coatings deposited by PVD and CVD techniques, Proceedings of the 11th International Scientific Conference on the Contemporary Achievements in Mechanics, Manufacturing and Materials Science CAM³S'2005, Gliwice-Zakopane, 2005 (CD ROM).